

A Collaborative Method for Positioning based on GNSS Inter Agent Range Estimation

Alex Minetto, Calogero Cristodaro, Fabio Dovis
 Department of Electronics and Telecommunications
 Politecnico di Torino
 Torino, Italy
 Email: *name.surname@polito.it*

Abstract—The limited availability and the lack of continuity in the service of Global Positioning Satellite Systems (GNSS) in harsh environments is a critical issue for Intelligent Transport Systems (ITS) applications relying on the position. This work is developed within the framework of vehicle-to-everything (V2X) communication, with the aim to guarantee a continuous position availability to all the agents belonging to the network when GNSS is not available for a subset of them. The simultaneous observation of *shared satellites* is exploited to estimate the Non-Line-Of-Sight Inter-Agent Range within a real-time-connected network of receivers. It is demonstrated the effectiveness of a hybrid localization algorithm based on the integration of standard GNSS measurements and linearised IAR estimates. The hybrid position estimation is solved through a self-adaptive iterative algorithm to find the position of receivers experiencing GNSS outages.

Index Terms—GNSS, ITS, Aided Positioning, Collaborative Localization, IAR.

I. INTRODUCTION

The limited availability and the lack of continuity in the GNSS services in harsh environment is a critical issues for many positioning-related applications. GNSS services typically fail or lose reliability when the satellites are not in Line-of-Sight (LOS), like in the presence of obstacles which partially or completely obstruct the satellite view. This work is focused on the non-continuity of satellite-based positioning service within typical urban environment. Such a phenomenon can be identified as critical aspects regarding to the rise of autonomous driving systems [1] and smart traffic management. During the last decades many solutions have been proposed and successfully implemented like loose and tight integration with generic Inertial Navigation System (INS) [2], [3], visual odometer [4], Light Detection and Ranging (LIDAR) [5] and Signal of Opportunity (SOP) exploitation [6]. Furthermore, the increasing interest in Cooperative Positioning (CP) [7],[8],[9], has shifted the research towards the implementation of smart computation strategies based on network distributed capabilities. Many advances have been also achieved about recent generation of robots and vehicles equipped with mass market GNSS receivers [10]. Furthermore, the recent open-access availability of raw data from mobile devices (i.e. smartphones) will soon allow to design collaborative algorithms just based on such a class of receivers. As anticipated, the typical scenario requires the integration of third-party devices which provide

additional measurements to mitigate service unavailability or to improve the positioning performance. To this aim, several ranging methods are available nowadays to determine range between two objects with a centemeter-level accuracy [11]. However, all ranging technologies are based on application-specific hardware and signal processing architectures for echo detection (e.g. RF radar, ultrasound sensor, wideband or ultra-wide band (UWB) ranging sensor) and they always require LOS condition. This paper preliminarily investigates a method for collaborative positioning with the aim to compensate for temporary unavailable GNSS service through GNSS receivers only. The proposed technique offers continuous position availability to all the agents belonging to a real-time connected network within harsh environments, exploiting last available position estimations. The Non-Line-Of-Sight (NLOS) Inter-Agent Range (IAR), exclusively based on GNSS pseudorange measurements and algorithmic data, is estimated and thus it is integrated as relative navigation data within a hybridized algorithm for positioning. Furthermore, IAR can be adopted for several purposes outside this specific application which will be further investigated in the future works.

II. PROBLEM FORMULATION

This section provides a detailed description of the proposed method. After introducing its general overview, the estimation of the IAR is presented from a geometrical point of view together with a mathematical description. Such a definition is tested in a realistic dynamic scenario to verify the effect of the uncertainties on the measurements. Finally, it is integrated within a hybrid algorithm for positioning which allows the *aided* agents to compute a new estimate of their positions.

A. Rationale of the IAR concept

The effect of outages during GNSS tracking operations typically returns an under-determined problem for the standard Position, Time and Velocity (PVT) algorithm. However, when two communicating receivers are observing and tracking the same satellite, two different correlated measurements are available about the same landmark (i.e. GNSS satellite). Urban and natural canyons or harsh environments in general show a high variability of the visible set of GNSS satellites from the point of view of a single receiver, while the joint multi-agent sky visibility is intuitively more complete and stable. Such

information is provided by the measured pseudoranges and the geometrical orientation represented by unitary pointing vectors computed iteratively within PVT algorithm [12]. By properly combining them, the IAR can be obtained as an additional piece of collaborative information. The IAR between each couple of receivers belonging to the network requires a run-time identification of all the simultaneously-visible satellites. Actually, the true positions of the receivers do not need to be explicitly shared and the LOS constraint of traditional techniques is also bypassed. In case of a scenario with an insufficient number of visible satellites for the PVT, a receiver can exploit such collaborative measurements in order to estimate its own position. The effectiveness of the technique has been verified by means of simulations by integrating the IAR as relative navigation data together with the reduced set of equations of standard PVT algorithms. Performance analysis is performed in terms of positioning error, given a set of communicating GNSS receivers in different sky visibility conditions.

B. IAR estimation

In order to provide a clear formalization of the theory, the following notation is used throughout the paper:

- k : time index
- \mathcal{N}_k : set of receivers in the network
- \mathcal{A}_k : subset of receivers out of GNSS service. $a \in \mathcal{A}_k$
- \mathcal{B}_k : subset of receivers under GNSS service. $b \in \mathcal{B}_k$
- \mathcal{J}_k : set of nominal visible satellites, $j \in \mathcal{J}$
- $\mathcal{G}_{k,a}, \mathcal{G}_{k,b} \subseteq \mathcal{J}_k$ subsets of visible satellites for the a -th and b -th receivers respectively
- $\mathcal{S}_{k,a,b} = \mathcal{G}_{k,a} \cap \mathcal{G}_{k,b}$: set of shared satellites which are simultaneously visible by a -th and b -th receiver, $s \in \mathcal{S}_{k,a,b}$.

For sake of simplicity, the elementary geometry shown in Figure 1 is considered. It depicts a static scenario with two ground GNSS receivers, namely the *aided* agent, a , and the *aiding* agent, b , and one shared satellite, s , is in LOS for both. All the theoretical results can be extended to an arbitrary number of receivers and shared satellites also in non-ideal dynamic scenario as further discussed in the next sections.

Suppose that \mathbf{x}_a and \mathbf{x}_b are the last estimated positions of a and b , they are defined as:

$$\mathbf{x}_i = [x_i, y_i, z_i], i \in [a, b]$$

and let s be the shared satellite, whose ECEF position is:

$$\mathbf{x}_s = [x_s, y_s, z_s], s \in \mathcal{S}$$

The satellite-to-receiver range is defined as:

$$\rho_{i,s} = \|\mathbf{x}_s - \mathbf{x}_i\| = \sqrt{(x_s - x_i)^2 + (y_s - y_i)^2 + (z_s - z_i)^2}$$

Let q be the cardinality of $\mathcal{G}_{k,i}$, H_i is defined, w.r.t. a linearisation point $\hat{\mathbf{x}}_0$, for the i -th receiver, as

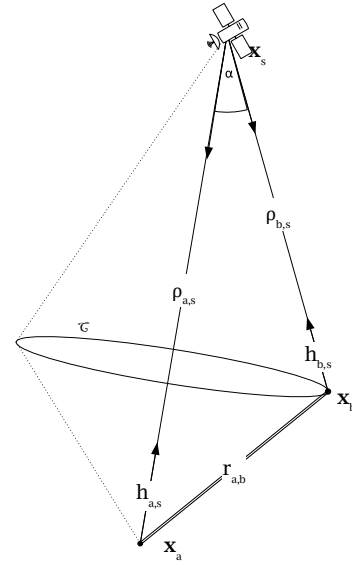


Fig. 1. Geometrical approach of GNSS-based range determination with description of ambiguity circumference as position protection of aiding agent

$$H_i = \begin{pmatrix} h_{1,x} & h_{1,y} & h_{1,z} \\ h_{2,x} & h_{2,y} & h_{2,z} \\ \vdots & \vdots & \vdots \\ h_{q,x} & h_{q,y} & h_{q,z} \end{pmatrix} \quad (1)$$

where each row describes the unitary vector defined as:

$$\mathbf{h}_{i,s} = \begin{bmatrix} \frac{x_i - \hat{x}_0}{\rho_{i,s}} & \frac{y_i - \hat{y}_0}{\rho_{i,s}} & \frac{z_i - \hat{z}_0}{\rho_{i,s}} \end{bmatrix} \quad (2)$$

The angle α between the two unitary vectors w.r.t. the shared-satellite s is computed as

$$\alpha = \arccos \left(\frac{\mathbf{h}_{a,s} \cdot \mathbf{h}_{b,s}}{|\mathbf{h}_{a,s}| \cdot |\mathbf{h}_{b,s}|} \right) \quad (3)$$

Finally, the IAR can be computed from a by solving the correspondent unknown side of the triangle, as shown in Figure 1, from the Carnot theorem as follows:

$$r_{a,b} = \sqrt{\rho_{a,s}^2 + \rho_{b,s}^2 - 2\rho_{a,s}\rho_{b,s} \cdot \cos(\alpha)}. \quad (4)$$

It is important to notice that, given α and $\rho_{b,s}$, the position of the *aiding* agent, \mathbf{x}_b , can be known to the *aided* agent a only with ambiguity because the orientation information is actually lost. It can be proved the dot product shown in Eq. (3) is not invertible since $\mathbf{h}_{i,s} \in \mathbb{R}^3$. The ambiguity circumference \mathcal{C} , shown in Figure 1, is the locus of points at distance $r_{a,b}$ from the receiver b and $\rho_{b,s}$ from the satellite s .

C. Heuristic analysis of uncertainties

In order to extend the IAR estimation to a realistic dynamic scenario, the effects of the non-ideal measurements are analysed. Noisy positions and pseudoranges are considered, whose errors are distributed according to zero-mean Gaussian distributions with properly defined variances [12]. In such a scenario, as depicted in Figure 2, the *aided* agent a does not reach a sufficient number of satellites in view to compute

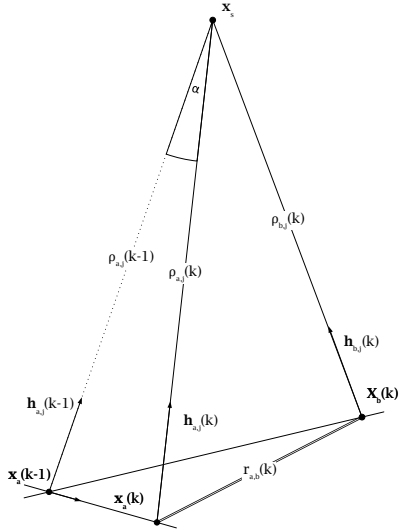


Fig. 2. Aided (a) and aiding (b) agents at instant k and $k-1$ by considering a dynamic scenario

the positioning solution at the instant k . It only holds the PVT result obtained at the previous instant $k-1$. As a basic analysis, the error introduced by the outdated fix is considered within the statistical distribution of the current position. At low speed, the displacement between two instant is small enough to make this assumption reasonable. The communication delay and the error due to outdated position are hence intrinsically considered within the σ_{UERE} of the aided agent. From a heuristic analysis, the following assumptions hold:

- the errors on \mathbf{x}_a and \mathbf{x}_b cause small fluctuations of the angle α due to the different order of magnitude between the IARs and the pseudoranges;
- the error on the IAR due to the small variations of α (i.e. σ_α) results negligible w.r.t. the error on the IAR due to the pseudoranges-related errors (i.e. σ_{UERE}). Notice that σ_{UERE} is the standard deviation nominally adopted to model the pseudorange error coefficient [12];
- when positioning solutions are i.i.d. it is possible to characterize the ratio between σ_{UERE} and σ_{IAR} as:

$$\gamma = \frac{\sigma_{UERE}}{\sigma_{IAR}} \sim \frac{1}{\sqrt{2}}$$

The trend of γ versus σ_{UERE} is plotted in Figure 3.

As a consequence of this remarks by referring to the theoretical analysis shown in Figure 4, the estimated IAR is defined as a random variable as follows:

$$\hat{r}_{a,b} = r_{a,b} + \epsilon_r \text{ where } \epsilon_r \sim \mathcal{N}(0, \gamma \cdot \sigma_{UERE}) \quad (5)$$

D. Hybridized positioning algorithm

The proposed hybridized positioning algorithm is based on the integration of standard GNSS pseudorange equations together with the estimated IAR measurements. It is proposed as a simple approach to validate the quality of the IAR

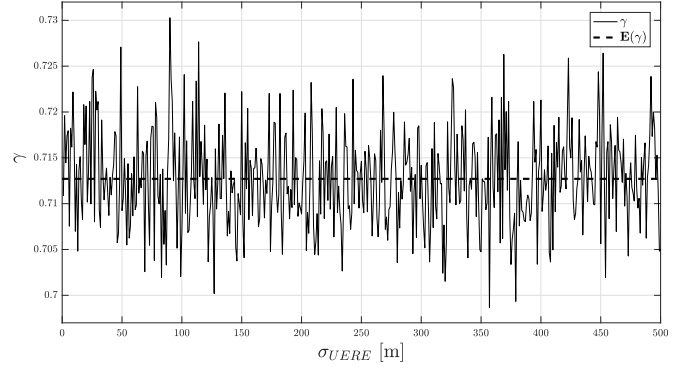


Fig. 3. γ versus σ_{UERE} varying agents positions error in [0-500] m

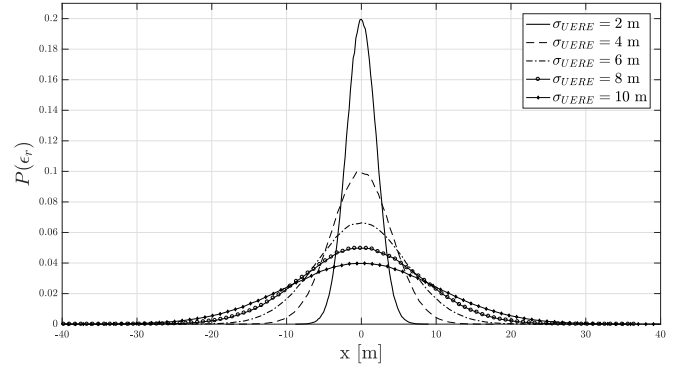


Fig. 4. Theoretical Probability Density Function of ϵ_r for i.i.d. positions distributions between two cooperating agents

estimation. Following the approach shown in work [13], in this paper, the interdependency between measurements is exploited by means of the integration of linearised IARs. PVT algorithm provides a positioning solution by iteratively solving the Least Mean Square for the linearised system [12].

$$\Delta \rho = H \Delta \mathbf{x} \quad (6)$$

Our solution provides the integration of the available IARs modifying (6) by means of matrix composition as:

$$\begin{bmatrix} \Delta \rho_{a,j} \\ \Delta r_{a,b} \end{bmatrix} = \begin{bmatrix} H_a \\ H_{IAR} \end{bmatrix} \times \Delta \mathbf{x} \quad (7)$$

where

$$\Delta \rho_{a,j} = \hat{\rho}_{a,j} - \rho_{a,j}, \Delta r_{a,b} = \hat{r}_{a,b} - r_{a,b}$$

The H_a matrix is calculated by the receiver a , for each instant, k , as shown in Eq. (1) whereas each row of matrix H_{IAR} is obtained through linearisation of IAR data as

$$\hat{h} = \begin{bmatrix} x_b - \hat{x}_0 & y_b - \hat{y}_0 & z_b - \hat{z}_0 \\ r_{x_0,b} & r_{x_0,b} & r_{x_0,b} \end{bmatrix} \quad (8)$$

where \mathbf{x}_0 must be the same as the linearisation point adopted for the definition of H_a . Hereafter, the composed coefficients matrix in Eq. (7) will be referred as \mathbf{H}_i .

By gathering all possible IARs and the relative linearisation coefficients from effective GNSS-referenced receivers in \mathcal{B} , the matrix \mathbf{H}_i , is assumed to be composed by reliable information.

Nevertheless, close *aiding* receivers can provide too strongly correlated data such that \mathbf{H}_i turns out to be an ill-conditioned matrix. In this case the quality of the estimated position may be very low. In fact, it is well known that linearised set of equations are very sensitive to linear dependence of matrix rows and to small perturbation of them [14]. The hybrid PVT algorithm presented, leads indeed to a typical ill-conditioned set of equations and it shows high instability of the convergence of the solution. An iterative algorithm proposed in [14] is adopted to enhance the convergence performance avoiding the inversion of the ill-conditioned $\mathbf{H}\mathbf{H}'$ product by means of a Self Adaptive Iterative Algorithm (SAIA) of Weighted Least Mean Square. For sake of completeness, the core steps of SAIA method are remarked here with a more familiar notation. As a general assumption, all the measurements (i.e. pseudoranges, IARs) are affected by Gaussian distributed errors as reasonably stated in the previous section.

$$\begin{cases} N = \mathbf{H}_i^T \mathbf{H}_i + \Lambda I \\ W = \mathbf{H}_i^T Y + \Lambda \mathbf{x}(k-1) \end{cases}$$

The perturbation parameter Λ is iteratively determined to accelerate the convergence. It must satisfy the condition $0 \leq \Lambda \leq 1$:

$$\begin{cases} \lambda = \min(|\text{eig}(\mathbf{H}_i^T \mathbf{H}_i)|) \\ \Lambda = \lambda \cdot 10^{0.5|\log_{10}(\lambda)|+1} \end{cases}$$

Z is calculated given the upper triangular matrix C obtained from the Cholesky decomposition of \mathbf{H}_i

$$CZ = W \quad (9)$$

and then \mathbf{x} is calculated solving the problem

$$C^T \mathbf{x} = Z \quad (10)$$

It has to be remarked that the solution \mathbf{x} is a differential vector with respect to the preceding approximation point and hence for each receiver $\hat{\mathbf{x}}_i = \mathbf{x}_0 - \mathbf{x}$.

The steps of the whole collaborative positioning algorithm can be summarised by the following pseudo-code.

Algorithm 1 Collaborative algorithm

- the *aided* agent **a** sends to the *aiding* agent **b** its last $\mathbf{h}_{a,s}$
 - **b** computes α applying (3)
 - **b** sends back α and its current $\rho_{b,s}$ to **a**
 - **a** estimates $r_{a,b}$ through Eq. (4)
 - **a** builds H by combining H_{IAR} and H_i
 - **a** computes its own position by solving Eq. (7)
-

III. SIMULATIONS AND RESULTS

In this section, some relevant results are reported to give an overall picture of the described positioning solutions. The method has been applied for a simulated urban environment with different combination of parameters.

The satellite ECEF positions of the subset \mathcal{J} are provided each second by a constellation simulator, based on real RINEX

TABLE I
PARAMETER OF SIMULATED SCENARIO

$ \mathcal{N} $	$ \mathcal{J} $	d_m	σ_{geo}	σ_{UERE}	f	r
40	6	10 m	1000 m	1 m	20	300

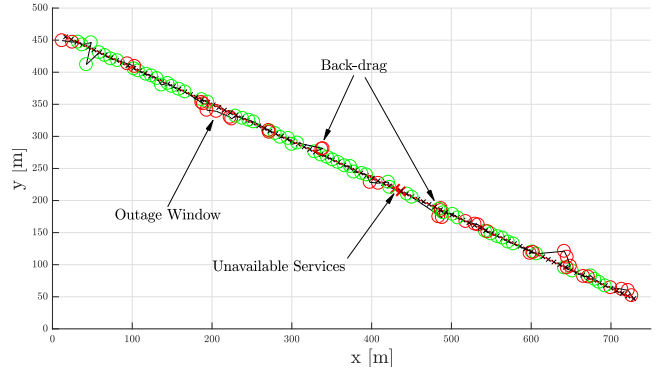


Fig. 5. Trajectory plot of a generic moving receiver in non-continuous GNSS service, red dots represent positions obtained from IAR-based solution while green ones are standard fixes from LMS PVT algorithm.

files, w.r.t. a given position (e.g. Turin, Italy) and epoch. From this reference location, the positions of the set of receivers \mathcal{N} is generated according to a Gaussian distribution centered around the reference with a standard deviation σ_{geo} . The satellites visibility from the receivers is determined by random transition of a binary matrix $V(k)$, every t_{int} seconds. *Aiding* agents for each lost receiver are then evaluated through the so called *cross-visibility matrix*, S . Thus collaborative NLOS IAR is calculated whenever it is needed. Once the equations are collected and processed, the \mathbf{H} matrix is defined for each receiver independently, thus iterating the SAIA algorithm for f iterations within the PVT algorithm performed for r iterations.

Rectilinear trajectories with no altitude variation are followed by the receivers belonging to the network. A realization of the process is depicted in Figure 5. Such a specific case is characterized by the parameters shown in Table I.

Standard PVT algorithm (green markers) and IAR-based positions (red markers) are used depending on either full ($i_i = 4$ satellites) or partial satellites visibility conditions, respectively. This actually demonstrates the good coherence and integrability of IAR with pseudorange measurements for outage mitigation purposes. The availability of the positioning service is increased along the path and the hybridized solutions are indeed well-distributed along the path although they show a higher variance of the error w.r.t. the GNSS estimates. Figure 5 clearly shows an effect, referred as back-drag, that can appear in case of implementation of IAR measurements. This is due to the integration of the outdated fix which makes the solution strongly conservative about the past of the motion showing backward located positions w.r.t. the true one. Predictions will be inspected as algorithm input in future works.

By looking at the position errors of a generic receiver versus time, as shown in Figure 6, it is possible to see how

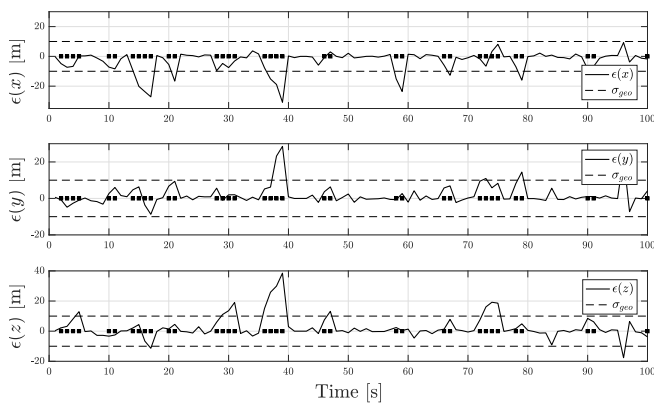


Fig. 6. Position errors of a generic simulated receiver in non-continuous GNSS availability, dots on x-axis represents nominally outage of service.

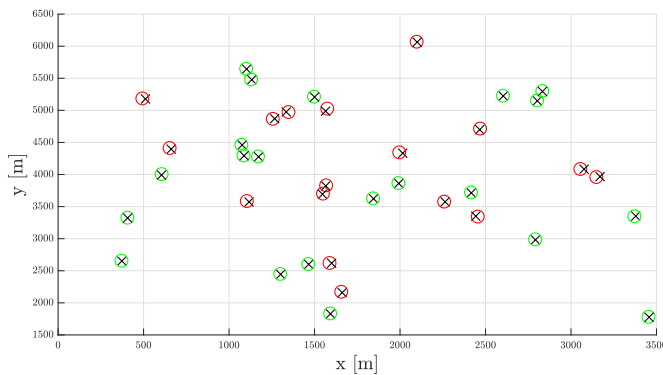


Fig. 7. Wide-range snapshot of GNSS-based estimates (green markers) and hybrid IAR-based estimates (red markers) vs. true positions of the receivers belonging to the network (black crosses).

the presence of contiguous outages causes a progressively higher bias along the trajectory. This behaviour is due to the increasing uncertainty in case of perpetuated IAR-based positioning. It can be remarked that the error on the final solution of the hybridized algorithm is limited and close to the error of the current true position with respect to the outdated fix. In Figure 7, a snapshot of the positions of all the receivers at a generic time instant is given. As shown, the estimation algorithm based on IAR (red circle) returns good convergence of positioning solution for all the *lost receivers*.

IV. CONCLUSION AND FUTURE RESEARCH

The $H(k-1)$ matrix is used to determine the IAR whenever a receiver belonging to the network experiences an outage. The hybrid solution successfully works in case of single failure guaranteeing the continuity of positioning service. Differently, the memory introduced in the process, in case of multiple faults, makes this solution intrinsically biased due to the error propagation in successive estimations and, despite to the fact that it guarantees a solution during epochs in which the standalone GNSS positioning would fail, it may lead to unacceptable results for a specific application. The results are indeed interesting by looking at the whole motion observation. The standard deviation $\sigma(\hat{\mathbf{x}})$ of the error on each axis, in

the case of few sequential outages, is typically bounded by the motion-induced error due to use of an outdated position. Future works will inspect more complex models for the motion of the receivers and a deeper theoretical analysis of the context-related variables which affects the reliability of IAR measurements (number of collaborating agents, number of available satellites, different motion speeds, etc.). Since the algorithm addresses dynamic frameworks, solutions based on Kalman Filters are being analysed to validate the strategy as a reliable option for integrating other additional ranging subsystems.

REFERENCES

- [1] J. Levinson and S. Thrun, "Robust vehicle localization in urban environments using probabilistic maps," in *Robotics and Automation (ICRA), 2010 IEEE International Conference on*. IEEE, 2010, pp. 4372–4378.
- [2] G. Falco, G. A. Einicke, J. T. Malos, and F. Dovis, "Performance analysis of constrained loosely coupled gps/ins integration solutions," *Sensors*, vol. 12, no. 11, pp. 15 983–16 007, 2012.
- [3] I. Miller, B. Schimpf, M. Campbell, and J. Leysens, "Tightly-coupled gps/ins system design for autonomous urban navigation," in *Position, Location and Navigation Symposium, 2008 IEEE/ION*. IEEE, 2008, pp. 1297–1310.
- [4] M. Schreiber, H. Königshof, A.-M. Hellmund, and C. Stiller, "Vehicle localization with tightly coupled GNSS and visual odometry," in *Intelligent Vehicles Symposium (IV), 2016 IEEE*. IEEE, 2016, pp. 858–863.
- [5] Y. Gao, S. Liu, M. M. Atia, and A. Noureldin, "Ins/gps/lidar integrated navigation system for urban and indoor environments using hybrid scan matching algorithm," *Sensors*, vol. 15, no. 9, pp. 23 286–23 302, 2015.
- [6] K. Pesyna, Z. Kassas, J. Bhatti, and T. Humphreys, "Tightly-coupled opportunistic navigation for deep urban and indoor positioning," in *Proceedings of the International Technical Meeting of The Satellite Division of the Institute of Navigation (ION GNSS)*, vol. 1, 2011, pp. 3605–3617.
- [7] F. Dovis, C.-F. Chiasserini, L. Musumeci, and C. Borgiattino, "Context-aware peer-to-peer and cooperative positioning," in *Localization and GNSS (ICL-GNSS), 2014 International Conference on*. IEEE, 2014, pp. 1–6.
- [8] M. A. Caceres, F. Penna, H. Wymeersch, and R. Garello, "Hybrid gnss-terrestrial cooperative positioning via distributed belief propagation," in *Global Telecommunications Conference (GLOBECOM 2010), 2010 IEEE*. IEEE, 2010, pp. 1–5.
- [9] R. Kurazume, S. Nagata, and S. Hirose, "Cooperative positioning with multiple robots," in *Robotics and Automation, 1994. Proceedings., 1994 IEEE International Conference on*. IEEE, 1994, pp. 1250–1257.
- [10] R. H. Ordóñez-Hurtado, W. M. Griggs, E. Crisostomi, and R. N. Shorten, "Cooperative positioning in vehicular ad-hoc networks supported by stationary vehicles," 2014.
- [11] F. de Ponte Müller, "Survey on ranging sensors and cooperative techniques for relative positioning of vehicles," *Sensors*, vol. 17, no. 2, p. 271, 2017.
- [12] E. Kaplan and C. Hegarty, *Understanding GPS: Principles and Applications*. Artech house, 2005.
- [13] S. Goel, A. Kealy, and B. Lohani, "Cooperative uas localization using lowcost sensors," *ISPRS Annals of Photogrammetry, Remote Sensing and Spatial Information Sciences*, vol. III-1, pp. 183–190, 2016.
- [14] X. Deng, L. Yin, S. Peng, and M. Ding, "An iterative algorithm for solving ill-conditioned linear least squares problems," *Geodesy and Geodynamics*, vol. 6, no. 6, pp. 453 – 459, 2015.